Article

Cell Reports

CD103$^+$ Dendritic Cells Control Th17 Cell Function in the Lung

Graphical Abstract

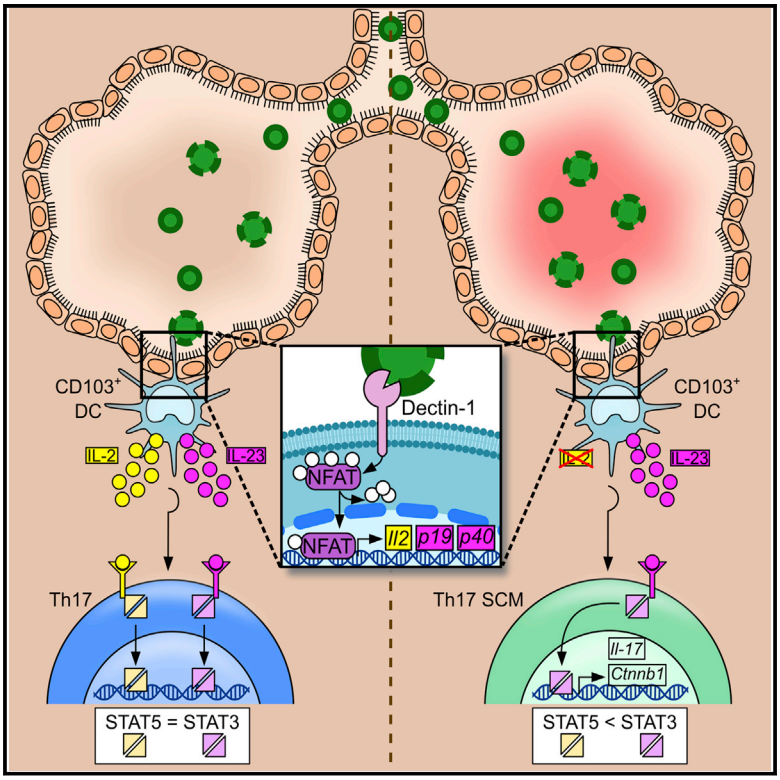

Authors

Teresa Zelante, Alicia Yoke Wei Wong, Tang Jing Ping, ..., Michael Poidinger, Paolo Puccetti, Paola Ricciardi-Castagnoli

Correspondence

teresa.zelante@unipg.it (T.Z.), paola.castagnoli@gmail.com (P.R.-C.)

In Brief

Th17 cells are characterized by plasticity, that is, an ability to acquire divergent functional capabilities. Zelante et al. report that, in pulmonary aspergillosis, lung CD103$^+$ dendritic cells shape the nature of the Th17 response via a finely tuned production of IL-2 dependent on phagocytosis and the Ca^{2+}-calcineurin-NFAT pathway.

Highlights

- *Aspergillus*-germinated morphotypes induce IL-2 in lung CD103$^+$ dendritic cells
- IL-2 production is dependent on the Ca^{2+}-calcineurin-NFAT pathway
- Deletion of dendritic-cell-derived IL-2 leads to higher mortality upon infection
- Dendritic-cell-derived IL-2 regulates Th17 cell phenotype

Accession Numbers

GSE58590

Zelante et al., 2015, Cell Reports *12*, 1789–1801
September 22, 2015 ©2015 The Authors
http://dx.doi.org/10.1016/j.celrep.2015.08.030

Cell Reports
Article

CD103$^+$ Dendritic Cells Control Th17 Cell Function in the Lung

Teresa Zelante,[1,2,*] Alicia Yoke Wei Wong,[1,3] Tang Jing Ping,[1] Jinmiao Chen,[1] Hermi R. Sumatoh,[1] Elena Viganò,[1] Yu Hong Bing,[1] Bernett Lee,[1] Francesca Zolezzi,[1] Jan Fric,[1,4] Evan W. Newell,[1] Alessandra Mortellaro,[1] Michael Poidinger,[1] Paolo Puccetti,[2] and Paola Ricciardi-Castagnoli[1,*]

[1]Singapore Immunology Network (SIgN), Agency for Science, Technology and Research (A*STAR), Singapore 138648, Singapore
[2]Department of Experimental Medicine, University of Perugia, 06132 Perugia, Italy
[3]National University of Singapore Graduate School for Integrative Sciences and Engineering, National University of Singapore, Singapore 117456, Singapore
[4]Integrated Center for Cell Therapy and Regenerative Medicine (ICCT), International Clinical Research Center, St. Anne's University Hospital Brno, Brno 65691, Czech Republic
*Correspondence: teresa.zelante@unipg.it (T.Z.), paola.castagnoli@gmail.com (P.R.-C.)
http://dx.doi.org/10.1016/j.celrep.2015.08.030

SUMMARY

Th17 cells express diverse functional programs while retaining their Th17 identity, in some cases exhibiting a stem-cell-like phenotype. Whereas the importance of Th17 cell regulation in autoimmune and infectious diseases is firmly established, the signaling pathways controlling their plasticity are undefined. Using a mouse model of invasive pulmonary aspergillosis, we found that lung CD103$^+$ dendritic cells (DCs) would produce IL-2, dependent on NFAT signaling, leading to an optimally protective Th17 response. The absence of IL-2 in DCs caused unrestrained production of IL-23 and fatal hyperinflammation, which was characterized by strong Th17 polarization and the emergence of a Th17 stem-cell-like population. Although several cell types may be affected by deficient IL-2 production in DCs, our findings identify the balance between IL-2 and IL-23 productions by lung DCs as an important regulator of the local inflammatory response to infection.

INTRODUCTION

In recent years, the view of Th17 cells as a short-lived, transient population has been overturned by data showing that, under some circumstances, they exhibit marked functional plasticity, multipotency, and a stem-cell-like phenotype (Muranski et al., 2011). In parallel, the contribution of the Th17/IL-17 response to both physiological and pathological inflammation has become well established (Korn et al., 2009). What remains unknown is which cellular interactions, factors, and signaling pathways determine the functional programs that are expressed by Th17 cells and how Th17 functionality is regulated under different conditions. One possible candidate is IL-2 (Boyman and Sprent, 2012). Because of the potency and pleiotropic roles of IL-2, the finding that myeloid dendritic cells (DCs) will produce the cytokine in response to microbial stimuli (Granucci et al., 2001; Wuest et al., 2011; Zelante et al., 2012) has posed intriguing questions about IL-2's role in the context of DC-T cell interactions.

After exposure to fungal antigens in vitro, DCs undergo an influx of Ca^{2+} that causes calcineurin, a Ca^{2+}-calmodulin-dependent phosphatase, to dephosphorylate nuclear factor of activated T cells (NFAT) in the cytoplasm, resulting in NFAT nuclear translocation and *Il2* transcription (Fric et al., 2014). We therefore asked what impact the absence of IL-2 in DCs would have on immune polarization and outcome of fungal infection by using a murine model of invasive pulmonary aspergillosis. Mice selectively lacking IL-2 in DCs expressed higher levels of IL-17 in their lungs during *Aspergillus fumigatus* infection and frequently died as a result of a pathological Th17 response. DCs that were not competent for IL-2 production would instead secrete IL-23, which drove fatal Th17-mediated immune pathology. These data suggest a crucial role for *Aspergillus*-induced IL-2 production by lung DCs that shapes the Th17 response to infection and determines disease resolution versus an ultimately fatal condition of hyperinflammation.

RESULTS

Aspergillus-Induced IL-2 Is Transcribed through a Ca^{2+}-Calcineurin-NFAT Pathway in DCs

Fungal β-glucan particles trigger IL-2 release from DCs (Rogers et al., 2005; Zelante et al., 2012). We first confirmed that whole fungal cells were also able to induce IL-2 in DCs in vitro. We exposed long-term growth-factor-dependent D1 cells—an immature murine myeloid CD103$^+$ CD11b$^+$ DC line (Winzler et al., 1997)—to different *Aspergillus* morphotypes, namely, conidia (A-con), partially germinated swollen conidia (A-sw), and fully germinated hyphae (A-hyp), as compared to whole-glucan particles (WGP). All morphotypes induced IL-2 release by D1 cells (Figure 1A). Although A-hyp was the strongest stimulus for IL-2 release, the physical properties of A-con and A-sw render them most suited to in vitro studies, and they were therefore used in the subsequent experiments. Exposure of D1 cells to A-con, and more so to A-sw, was marked by a cytosolic Ca^{2+}

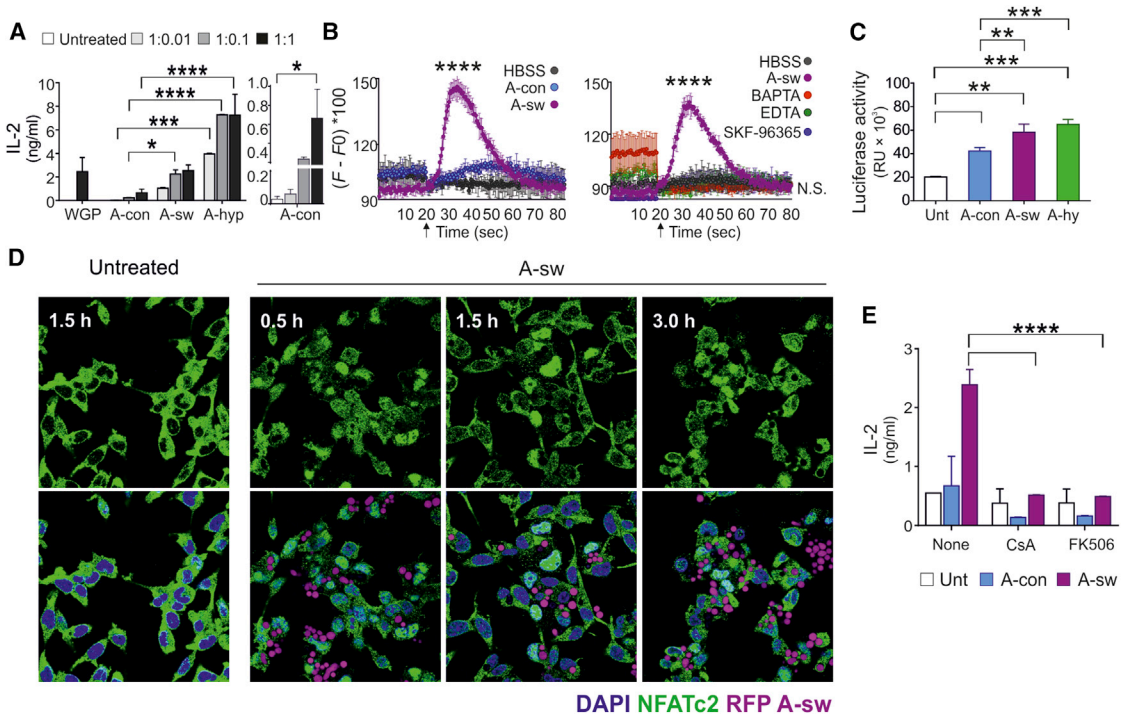

Figure 1. IL-2 Is Transcribed through a Ca^{2+}-calcineurin-NFAT-Signaling Pathway in Response to *Aspergillus* Morphotypes

(A) ELISA of IL-2 in supernatants from D1 cells exposed to *Aspergillus* for 8 hr at cell-to-fungal morphotype ratios of 1:0.01, 1:0.1, and 1:1 or to WGP (10 μg/ml).

(B) Ca^{2+} flux in D1 cells at cell-to-fungal morphotype ratios of 1:1 or 1:0.1. BAPTA (20 μM) and SKF-96365 (10 μM) were added 1 hr prior to fungal exposure to deplete intracellular Ca^{2+} and inhibit the store-operated channels, respectively. EDTA (4 mM) was added for the last 45 min of incubation in combination with Fluo4-AM. Values (*F*) were normalized to baseline reading at the first time point (*F*0) after the injection of the stimuli, and percentage (*F*/*F*0*100) is shown. Data are from one experiment representative of three (means ± SD of triplicate cultures are shown).

(C) Luciferase activity, indicating NFAT nuclear translocation, was measured in NFAT translocation-firefly luciferase reporter cells.

(D) Immunofluorescent images showing NAFTc2 (green), cell nuclei (blue, DAPI) and RFP A-sw (magenta) in D1 cells. Magnification is at 100×. Results are representative of three experiments. Quantitative analysis of the frequency of NFATc2 nuclear localization is presented in Figure S1A.

(E) ELISA of IL-2 from D1 cells exposed to *Aspergillus* for 8 hr at cell-to-fungal morphotype ratios of 1:0.1. D1 cells were treated with CsA and FK506 for 1 hr before stimulation with *Aspergillus*. Means ± SD of triplicate cultures are shown.

*p < 0.05; **p < 0.01; ***p < 0.001; and ****p < 0.0001 (ANOVA with Bonferroni post-test). See also Figure S1.

influx (Figure 1B, left panel). Pre-incubating D1 cells with EDTA to chelate extracellular Ca^{2+}, or the cell-permeant Ca^{2+} chelator BAPTA, revealed a role for both extracellular and intracellular Ca^{2+} stores. Moreover, the addition of SKF-96365, which inhibits Ca^{2+}-release-activated channels (CRACs) (Hsu et al., 2001), similarly abrogated Ca^{2+} influx in response to *Aspergillus* exposure in D1 cells (Figure 1B, right panel).

Exposure to all morphotypes induced nuclear translocation of NFAT, measured by an NFAT-luciferase reporter assay, with the greatest luciferase activity recorded in response to germinated fungi (Figure 1C). In D1 cells exposed to A-sw, NFAT nuclear translocation was detected by immune-fluorescence microscopy at 0.5–3 hr (Figures 1D and S1A).

IL-2 production by D1 cells exposed to A-sw depended on NFAT signaling, as treatment with the calcineurin B inhibitors cyclosporin A (CsA) or tacrolimus (FK506) significantly reduced the amount of IL-2 in culture supernatants (Figure 1E). Consistent with a need for fungal uptake, the inhibition of actin polymerization with cytochalasin D revealed the parallel importance of phagocytic function in D1 cells for IL-2 production (Figure S1B). Finally, IL-2 release did not require the MyD88-TRIF signaling complex but was instead contingent on dectin-1, which initiates Ca^{2+}-calmodulin-dependent events in response to β-glucan (Figures S1C and S1D).

The NFAT family of transcription factors has emerged as a key mediator of the initiation of immune responses, and specifically, NFATc2 is known to mediate the transcription of IL-2 released by DCs in response to LPS upon Ca^{2+} entry (Zanoni et al., 2009). To establish whether NFATc2 was acting directly or indirectly in modulating IL-2 production, we performed a chromatin immunoprecipitation (ChIP) assay in D1 cells. In the absence of a commercially available NFATc2 antibody suitable for use in ChIP assays, we devised a V5-tagging approach (Yu et al., 2011) (Figure S1E). This confirmed that NFATc2 bound the promoter region of *Il2* upon WGP stimulation of D1 cells (Figure S1E), which is consistent with our recent finding that NFATc2 occupancy is responsible for curdlan-mediated activation of multiple genes in DCs (Yu et al., 2015).

Thus, *A. fumigatus* fungal morphotypes trigger IL-2 release from murine myeloid DCs through the receptor dectin-1, phagocytosis, and the downstream Ca^{2+}-calmodulin-dependent NFAT signaling pathway.

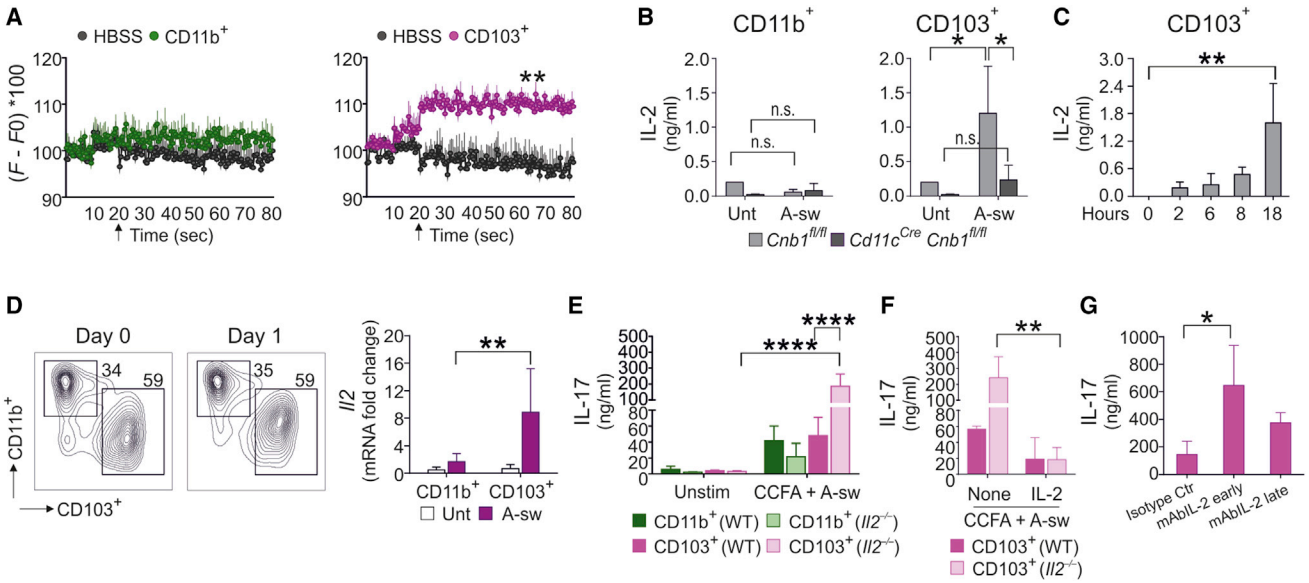

Figure 2. CD103$^+$ DC-Derived IL-2 Regulates Th17 Differentiation In Vitro in Response to *Aspergillus*

(A) Ca^{2+} flux in sorted populations of lung DCs from WT mice following exposure to A-sw at cell-to-fungal morphotype ratio of 1:0.1. Data are from one experiment representative of three (means ± SD of triplicate cultures). **p < 0.01 (Student's t test).

(B) ELISA of IL-2 in CD103$^+$ or CD11b$^+$ lung DCs isolated from *Cnb1*$^{fl/fl}$ or *Cd11c*^{Cre} *Cnb*$^{fl/fl}$ mice after incubation with A-sw for 18 hr at a cell-to-fungal morphotype ratio of 1:0.1. *p < 0.05 (Student's t test).

(C) ELISA of IL-2 in supernatants of CD103$^+$ lung DCs isolated from *Cnb1*$^{fl/fl}$ mice after incubation with A-sw for the time points indicated, at cell-to-fungal morphotype ratio of 1:0.1. **p < 0.01 (Student's t test).

(D) Representative flow cytometry plots of CD11b and CD103 expression within the total lung DC population at day 0 and day 1 following intranasal inoculation with heat-inactivated A-sw (left panel) and qRT-PCR analysis of *Il2* mRNA expression in lung DC subpopulations isolated from untreated (Unt) mice or mice inoculated intranasally with heat-inactivated A-sw 1 day post-inoculation (right panel).

(E) ELISA of IL-17 in supernatants of WT CD103$^+$ or CD11b$^+$ lung DC-T cell co-cultures. DCs were incubated overnight with heat-inactivated A-sw (cell-to-fungal morphotype ratio of 1:0.1) and CCFA (10 μg/ml).

(F) The day after, 1 × 10^6/ml CD4$^+$ T cells from CCFA-immunized mice (see Experimental Procedures) were added at a ratio of 1 DC to 20 T cells without or with the addition of 10 ng of IL-2. On day 6, ELISA of IL-17 was performed.

(G) CD103$^+$ lung DCs from WT C57BL/6 mice were incubated with heat-inactivated A-sw and CCFA overnight and with or without anti-IL-2 (10 μg/ml; early). 1 × 10^6/ml CD4$^+$ T cells from CCFA-immunized mice were added at a ratio of 1 DC to 20 T cells, with or without anti-IL-2 (10 μg/ml; late).

*p < 0.05; **p < 0.01; and ****p < 0.0001 (ANOVA with Bonferroni post-test). See also Figure S2.

Lung CD103$^+$ DC-Derived IL-2 Inhibits Th17 Cell Polarization

Several subpopulations of murine lung DCs are present in the steady state: "classical" CD11c$^+$ DCs (encompassing CD103$^+$ [type 1] and CD11b$^+$ [type 2] DC subsets) and plasmacytoid DCs (Guilliams et al., 2014). Recent data suggest that CD11b$^+$ DCs are essential for T-helper cell priming in aspergillosis (Schlitzer et al., 2013), and pulmonary CD103$^+$ DCs have an established role in the response to particulate antigens (Greter et al., 2012); however, it is unknown whether any of those subpopulations are able to release IL-2 and whether NFAT proteins are important in their signaling pathways.

We generated mice conditionally lacking the calcineurin B1 subunit (CnB) in the CD11c$^+$ DC population (*Cd11c*^{Cre} *Cnb*$^{fl/fl}$ mice; see Experimental Procedures). CD11c$^+$ DCs were isolated from the lungs of *Cd11c*^{Cre} *Cnb*$^{fl/fl}$ mice and the CD11b$^+$ and CD103$^+$ subpopulations then exposed to A-sw ex vivo. A substantive Ca^{2+} flux was only observed in the CD103$^+$ fraction (Figure 2A), and it was accompanied by a significant induction of IL-2 in response to A-sw (Figure 2B), which accumulated in culture medium over the following 18 hr (Figure 2C). Moreover, CD103$^+$ DCs from the lungs of *Cd11c*^{Cre} *Cnb*$^{fl/fl}$ mice had markedly diminished IL-2 responses to A-sw (Figure 2B). These results confirmed that, similar to our observations in D1 cells, CD103$^+$ DCs from mouse lung transcribe *Il2* in an NFAT pathway-dependent manner following exposure to A-sw ex vivo.

We asked whether *Il2* expression also occurred in lung DCs from wild-type (WT) mice during acute aspergillosis. Mice were exposed intranasally to A-sw, and after 1 day, DC subpopulations were sorted from dissociated lung tissue. We found that *Il2* mRNA was selectively induced in CD103$^+$ DCs (Figure 2D). Interestingly, whereas lung CD11b$^+$ DCs also expressed the calcineurin (*Ppr1*) and *Nfat1* genes (Figure S2A), they were evidently unable to produce IL-2. Further investigation of their transcriptional profile revealed significantly lower levels of *Sept4* expression in response to *Aspergillus* relative to the CD103$^+$ fraction (Figure S2B). Septin4 is essential for store-operated Ca^{2+} entry organization and therefore required for NFAT translocation (Sharma et al., 2013), thereby likely explaining/contributing to the absence of *Il2* induction in those cells.

Because of the IL-2 production from CD103$^+$ lung DCs ex vivo—which is associated with *Il2* expression in vivo—we investigated

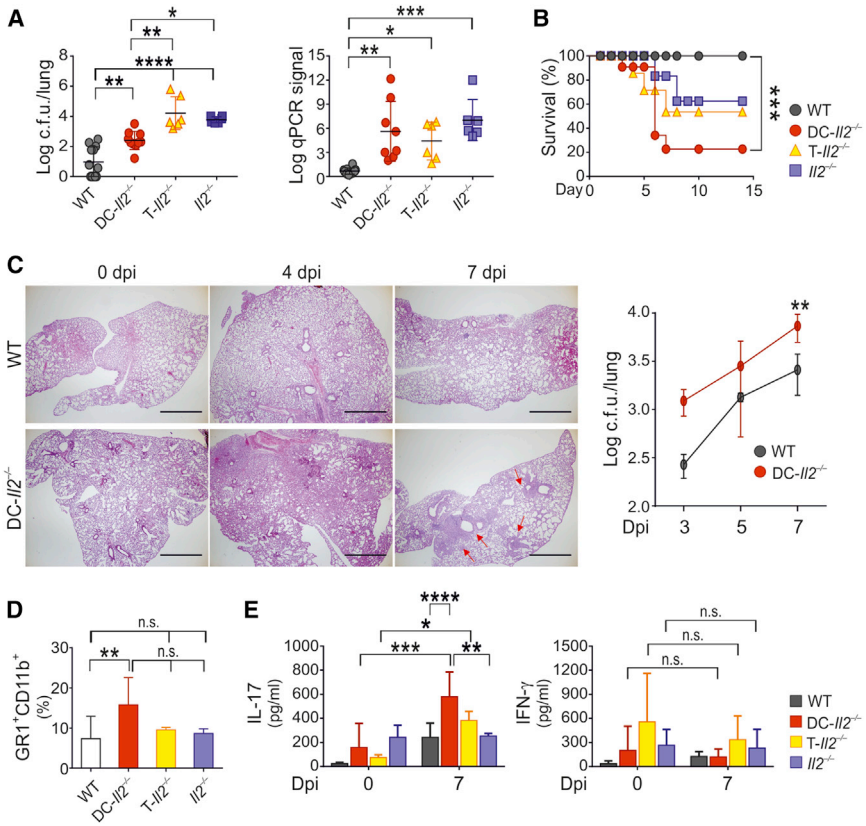

Figure 3. Mice with Deficiency of IL-2 in DCs Are Highly Susceptible to Invasive Aspergillosis

WT, DC-*Il2*$^{-/-}$, T-*Il2*$^{-/-}$, or *Il2*$^{-/-}$ mice were infected intranasally with *Aspergillus* and monitored for 7 days.

(A) *Aspergillus* CFU/lung and 18S rRNA gene expression measured by qPCR; *p < 0.05; **p < 0.01; ***p < 0.001; and ****p < 0.0001 (ANOVA with Bonferroni post-test).

(B) Survival rate; ***p < 0.001 (log rank test).

(C) H&E-stained lung sections with arrows indicating mononuclear cell infiltration occluding the airways; original magnification, 4×; scale bar, 1,000 μM (right panel); CFU/lung at 3, 5, and 7 days post-infection; **p < 0.01 (two-tailed Student's t test; left panel).

(D) Flow cytometric analysis of frequency of GR1$^+$ CD11b$^+$ cells in the pulmonary cells of mice at 7 days post infection. **p < 0.01 (ANOVA with Bonferroni post-test).

(E) ELISA of IL-17 and IFN-γ in supernatants of whole-lung homogenates at day 0 and 7 days post-infection; data were normalized to total protein (t.p.) content; *p < 0.05; **p < 0.01; ***p < 0.001; and ****p < 0.0001 (ANOVA with Bonferroni post-test).

See also Figures S3 and S4.

the role of those events in aspergillosis. As IL-2 is crucial for Th cell differentiation (Malek, 2008), we first asked whether T cell polarization differed in mice lacking DC-derived IL-2. Inguinal, popliteal, and para-aortic lymph node CD4$^+$ T cells from mice immunized with *A. fumigatus* crude culture filtrate antigens (CCFA) (Grünig et al., 1997) were cultured with GM-CSF bone-marrow-derived DCs (GM-DCs), either from WT mice or from mice lacking IL-2 in all tissues (i.e., *Il2*$^{-/-}$ mice). In vitro proliferative responses of T cells isolated from immunized mice and stimulated with CCFA (Figure S2C) were significantly lower when GM-DCs lacked the ability to produce IL-2 (Figures S2D and S2E).

Using pulmonary CD103$^+$ DCs and CD11b$^+$DCs, we investigated the effect of IL-2 deficiency on Th cell polarization. After overnight incubation of lung DC subsets with A-sw and CCFA to allow full induction of DC IL-2 production (as revealed by the kinetics in Figure 2C), DCs were co-cultured with T cells isolated from immunized mice (Figure 2E). The absence of IL-2 in pulmonary CD103$^+$ DCs led to a significantly higher IL-17 production relative to culturing T cells with IL-2-competent DCs (Figure 2E). This effect was directly attributable to the absence of IL-2, as adding recombinant IL-2 to cultures containing *Il2*$^{-/-}$ CD103$^+$ DCs significantly reduced IL-17 production from co-cultured T cells (Figure 2F). To confirm that DCs and not T cells were the critical source of IL-2, we added anti-IL-2 antibodies (or an isotype control) to cultures either before (Figure 2G, early) or after (Figure 2G, late) including T cells. Increased IL-17 production was selectively induced by adding anti-IL-2 at the time of DC priming with antigen, in the absence of T cells (Figure 2G). Thus, *Il2*—transcribed through a Ca^{2+}-calcineurin-NFAT-signaling pathway in CD103$^+$ DCs—modulated Th17 cell expansion in vitro in response to *Aspergillus*-germinated particles.

Lung DC-Derived IL-2 Controls Lung Inflammation and Susceptibility to Invasive Aspergillosis

Optimally balanced Th17 functionality in response to fungal antigens is required for resolution of invasive pulmonary aspergillosis (Romani et al., 2008). To assess the impact of DC-derived IL-2 deficiency in vivo, we also generated mice conditionally lacking *Il2* in the CD11c$^+$ DC population (*Cd11c*^{Cre} *Il2*$^{fl/fl}$ mice; see Figures S3A–S3C). We compared the *Cd11c*^{Cre} *Il2*$^{fl/fl}$ mice bearing a selective deficiency of IL-2 in CD11c$^+$ DCs (DC-*Il2*$^{-/-}$) with mice lacking IL-2 in all tissues (*Il2*$^{-/-}$) or lacking IL-2 expression in CD4$^+$ T cells (T-*Il2*$^{-/-}$), as well as with WT mice.

We selected *Cd11c*^{Cre} *Il2*$^{fl/fl}$ mice with specific targeted deletion in DCs, where T cells and DCs had comparable secretion of IL-2 in response to thapsigargin (60 nM) relative to WT T cells (Figure S3D). Mice of each genotype were infected intranasally with *A. fumigatus*, resulting in invasive pulmonary aspergillosis. Clinical signs of the disease were obvious in all groups at 7 days post-infection. However, significantly higher fungal loads and *Aspergillus* 18S expression in the lungs were observed in the three mutant strains than in WT animals (Figure 3A). Despite the fact that *Il2*$^{-/-}$ and T-*Il2*$^{-/-}$ mice had significantly higher fungal burdens in their lungs than DC-*Il2*$^{-/-}$ mice, they frequently survived longer than did animals selectively lacking IL-2 in DCs, 80% of which would succumb to challenge by day 6 of infection (Figure 3B). This indicated that fungal load was not, per se, the

major determinant of disease outcome and that IL-2 production by lung DCs contributed substantially to overall protection. Whereas either generalized or T-cell-confined IL-2 deficiency increased local invasiveness by *Aspergillus*, selective lack of IL-2 in lung-resident DCs appeared to trigger an acute and potentially fatal effect not directly attributable to an increased fungal burden in the lungs.

Kinetic analysis of fungal load during the first week post inoculation with *Aspergillus* revealed a consistent trend of exacerbated infection in DC-*Il2*$^{-/-}$ mice from day 3, which was maximal at 7 days (Figure 3C). Histopathology revealed multifocal bronchoalveolar histiocytic pneumonia and a greater multifocal perivascular neutrophil infiltration compared to WT (Figure 3C), T-*Il2*$^{-/-}$, or *Il2*$^{-/-}$ mice (Figure S4A). Differences in cellular infiltrates among genotypes were not due to global changes in immune cell composition, as DC-*Il2*$^{-/-}$ mice had CD4^{+} and CD8^{+} T cell frequencies in their lungs and spleens similar to those in WT mice (Figure S4B). Considering innate immune cells, only the frequency of GR1^{+} CD11b^{+} neutrophils was significantly higher in the lungs of DC-*Il2*$^{-/-}$ mice (Figures 3D and S4C).

IL-17 and IFN-γ are secreted in mice with pulmonary *Aspergillus* infections (Romani, 2011), and they have a potential for contributing to resolution of infection as well as causing severe tissue inflammation. Mice were inoculated with A-con, and 7 days later, the cytokine content of their lung homogenates was measured by ELISA, which revealed that DC-*Il2*$^{-/-}$ mice produced significantly higher amounts of IL-17 than did their WT counterparts. Lung-associated IFN-γ was equally expressed across the four genotypes (Figure 3E). Therefore, lung DC-derived IL-2 seemed to control lung inflammation and susceptibility to invasive aspergillosis by regulating the IL-17 response.

Lung DC-Derived IL-2 Controls the Th17 Cell Response In Vivo

Because IL-2 is known to control T-reg cell survival (Fontenot et al., 2005) and one function of T-reg cells is to restrain pathological inflammation, we investigated whether the abundance of Foxp3^{+} CD4^{+} T-reg cells varied in mice of the different genotypes. The relative frequencies of Foxp3^{+} CD4^{+} T cells in the lungs and thoracic lymph nodes (TLNs) of DC-*Il2*$^{-/-}$ and WT mice were similar, regardless of any exposure to intranasal *Aspergillus* (Figure 4A). mRNA expression of *Foxp3* in T cells did not change during infection (Figure 4B). Although not statistically significant, T-*Il2*$^{-/-}$ and *Il2*$^{-/-}$ mice had lower T-reg-cell-associated *Foxp3* expression in their lungs (Figure 4C) and splenic (Figure S4D) CD4^{+} T cell compartments than did WT and DC-*Il2*$^{-/-}$ animals.

In agreement with the pattern of cytokine production seen in lung homogenates (Figure 3E), flow cytometry analysis of freshly harvested, inflammatory CD45^{+} cells from the lungs revealed a higher frequency of IL-17-producing cells in DC-*Il2*$^{-/-}$ mice infected with *Aspergillus* relative to WT counterparts (Figure 4D). The increased IL-17 expression in the lungs of DC-*Il2*$^{-/-}$ mice was entirely attributable to CD45^{+} CD90^{+} cells (Figure 4E), which were still present at 14 days of infection in the lungs from DC-*Il2*$^{-/-}$ mice (Figure 4F), but not in TLNs from the same animals (Figure 4E). CD90^{+} IL-17^{+} cells were not detected in the lungs of T-*Il2*$^{-/-}$ and *Il2*$^{-/-}$ mice or of WT animals (Figure 4G). Because both innate lymphoid cells (ILCs) and T cells in the lung express the cell surface marker CD90, CD90^{+} IL-17^{+} cells were further examined for their expression of other T cell markers. The analysis revealed that 70% of the population expressed CD3, with 60% expressing CD4 and 9% expressing CD8 (Figure 4H). Collectively, these data demonstrated that IL-2 produced by lung DCs was responsible for the increased frequency of IL-17^{+} CD45^{+} CD90^{+} T cells late in infection with *Aspergillus*.

High-Dimensional-Analysis-Based Profiling of Lung T Cells Expanded in DC-*Il2*$^{-/-}$ Mice

We investigated the nature of the pulmonary immune cells responsible for the shift toward a predominantly pathogenic IL-17 response under conditions of DC-derived IL-2 deficiency. We used a recently developed technique, single-cell mass spectrometric cytometry by time-of-flight (CyTOF mass cytometer), which is a unique means of characterizing phenotypically and functionally heterogeneous lymphocyte populations (Bandura et al., 2009; Newell et al., 2012). Using a panel of heavy metal isotope-labeled antibodies recognizing numerous surface and soluble molecules expressed by lung immune cells, we simultaneously analyzed the expression of 25 markers (Table S1). CD45^{+} CD90^{+} cells were also examined in detail (Figure 5A). Mass cytometry analysis revealed that pulmonary T cells naturally cluster into distinct subsets according to the presence of CD4 and CD8 on the cell surface (Figure 5B).

We employed density-based clustering using support vector machine technology to improve the efficiency of image grouping so to result in grouped images being assigned to different clusters. We first reduced the dimensionality to 2D using t-SNE (Becher et al., 2014). On the t-SNE map, we generated a density plot from which we identified density peaks. Cells located in the neighborhood of each density peak were classified to clusters represented by their respective peaks. Cells resulting as otherwise unclassified were assigned by using support vector machine. DC-*Il2*$^{-/-}$ mice expressed clusters 10, 6, 9, and 4 to a greater extent than did WT mice (Figure 5C). The frequency of T cell marker expression in the different clusters is graphically represented as a heatmap (Figure 5D). Interestingly, the T cell subsets were clustered similarly in the lungs of T-*Il2*$^{-/-}$ and *Il2*$^{-/-}$ mice but to a different extent as compared to DC-*Il2*$^{-/-}$ mice (Figures S5A–S5C). Because clusters upregulated in DC-*Il2*$^{-/-}$ mice were all Sca1^{+}, we concluded that *Aspergillus*-infected DCs affect the T cell differentiation status in the lung by releasing IL-2 after infection.

As both ILC2 and ILC3 subsets in the lung also express Sca1 and CD90, it is possible that IL-2 derived from DCs might additionally impact these populations. With this in mind, we explored the impact of DC-restricted IL-2 deficiency in *Rag2*$^{-/-}$ mice, which completely lack mature lymphocytes but possess ILCs. We compared *Rag2*$^{-/-}$ mice with DC-*Il2*$^{-/-}$ *Rag2*$^{-/-}$ mice and asked whether we could detect ILC2 or ILC3 expansion in the absence of T cells. We did not observe any increase in frequency of lung IL-17^{+} CD45^{+} CD90^{+} cells in either *Rag2*$^{-/-}$ or DC-*Il2*$^{-/-}$ *Rag2*$^{-/-}$ at 7 days of inoculation with *Aspergillus* (Figure 5E), indicating that the effects of DC-derived IL-2 on the IL-17^{+}

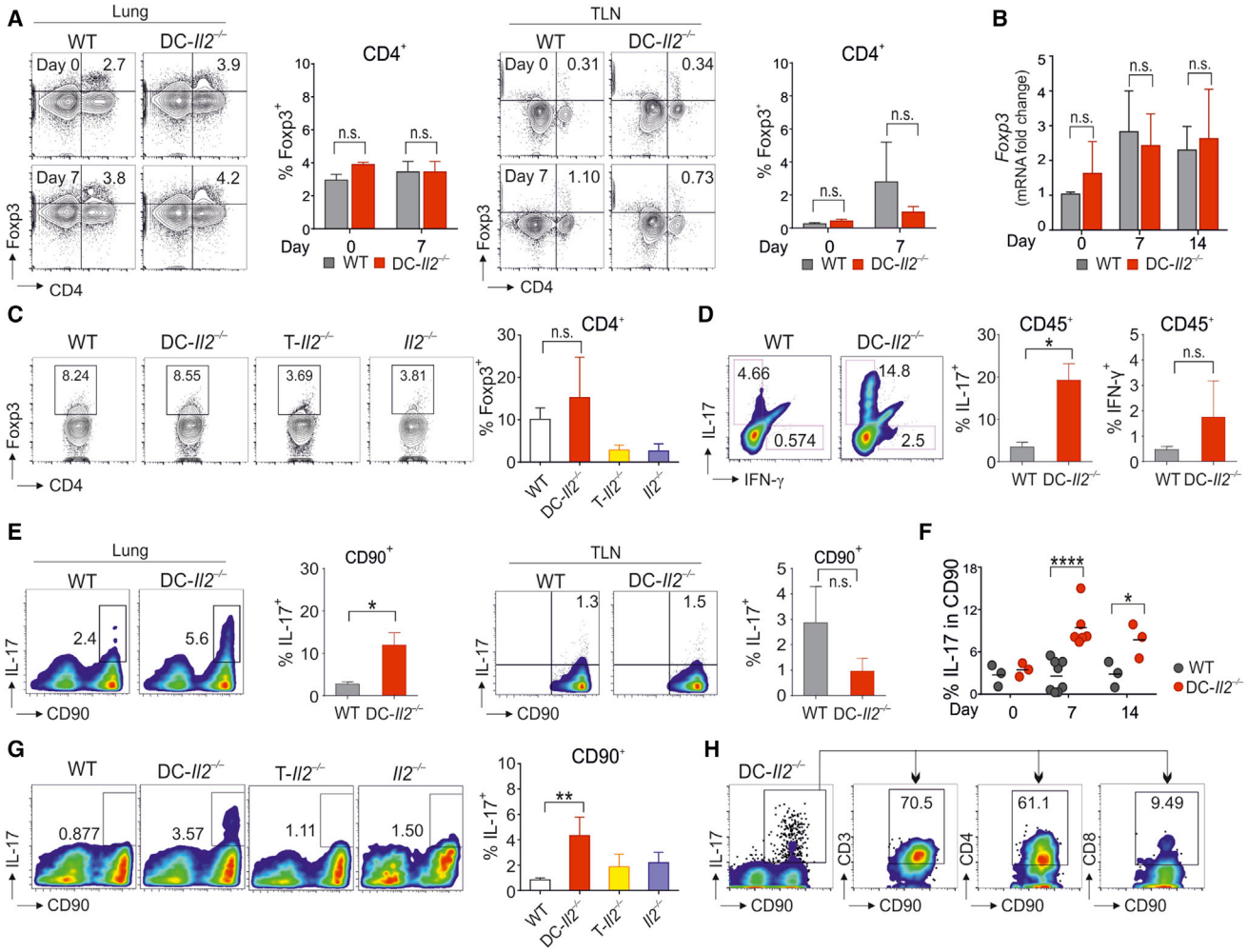

Figure 4. Lung DC-Derived IL-2 Controls IL-17$^+$CD45$^+$CD90$^+$CD3$^+$CD4$^+$ T Cell Expansion In Vivo

WT, DC-*Il2*$^{-/-}$, T-*Il2*$^{-/-}$, or *Il2*$^{-/-}$ mice were inoculated intranasally with *Aspergillus*.

(A) Representative contour plots among lung and thoracic lymph node (TLN) cells. Bar graphs show the percentage of CD4$^+$ T cells that expressed Foxp3, from three independent experiments (means ± SD).

(B) Fold change in *Foxp3* expression in CD4$^+$ T cells at 7 and 14 days post-infection. Data are normalized to abundance of transcripts for the housekeeping gene *Gadph* and presented relative to WT mice on day 0 (means ± SD).

(C) Representative contour plots of Foxp3 and CD4 expression in lung-gated CD4$^+$T cells upon infection at day 7. Bar graphs show the percentage of CD4$^+$ T cells that expressed Foxp3, from three independent experiments.

(D) Pseudocolor plots of intracellular IL-17 and IFN-γ in CD45$^+$ lung cells at day 7 post-infection. Bar graphs show the percentage of CD4$^+$ T cells that expressed IL-17 or IFN-γ, from three independent experiments.

(E) Representative pseudocolor plots of IL-17 and CD90 expression within CD45$^+$ cells from lungs and TLNs at day 7 post-infection.

(F) Percentage of CD90$^+$ lung T cells that express IL-17 on days 0 (uninfected), 7, and 14 of *Aspergillus* infection. *$p < 0.05$ (Student's t test), ****$p < 0.0001$ (ANOVA with Bonferroni post-test).

(G) Representative pseudocolor plots of IL-17 and CD90 expression within CD45$^+$ cells from lungs of indicated mice at day 7 post-infection. Bar graphs show the percentage of CD45$^+$ CD90$^+$ cells that expressed IL-17, from three independent experiments. **$p < 0.01$ (ANOVA with Bonferroni post-test).

(H) Representative pseudocolor plot showing detailed phenotypic characterization of the IL-17$^+$ CD90+ lung cell population in DC-*Il2*$^{-/-}$ mice at day 7 post-infection (means ± SD). In addition, gated IL-17$^+$ CD90$^+$ lung cells were analyzed to determine the percentage of cells co-expressing CD3, CD4, and CD8. Results are representative of three independent experiments.

Also see Figure S4.

CD45$^+$ CD90$^+$ CD3$^+$ cell compartment are mostly confined to T cells and do not affect ILCs.

Because DC-*Il2*$^{-/-}$ *Rag2*$^{-/-}$ mice did not show any expansion of IL-17$^+$ CD45$^+$ CD90$^+$ CD3$^+$ T cells in response to *Aspergillus*, we wanted to analyze the susceptibility of DC-*Il2*$^{-/-}$ *Rag2*$^{-/-}$ mice to fungal infection. At 7 days of infection, these mice showed neither higher colonization nor increased mortality relative to *Rag2*$^{-/-}$ counterparts (Figure 5F).

Taken together, these data showed that the IL-17$^+$ CD45$^+$ CD90$^+$ CD3$^+$ T cells—which were expanded in T cell-sufficient

DC-*Il2*$^{-/-}$ mice—directly contributed to the lung pathology in invasive aspergillosis. These results also confirmed previous data showing that, in acute phases post-infection, the role of IL-17$^+$ CD3$^+$ T cells in the lung mostly contributes to exacerbating disease (Zelante et al., 2007).

DC-Derived IL-2 Prevents Th17 Pathogenic Signature

To further analyze the phenotype of IL-17$^+$ CD45$^+$ CD90$^+$ CD3$^+$ T cells in DC-*Il2*$^{-/-}$ mice, we used contour plots of mass cytometry data, with IL-17A$^+$ cells being gated and superimposed on the t-SNE map of pulmonary CD45$^+$ CD90$^+$ cells from WT and DC-*Il2*$^{-/-}$ mice (Figure 6A). Contour plot cluster analysis indicated a greater abundance of cluster-9 IL-17-producing cells in DC-*Il2*$^{-/-}$ mice than in WT mice (Figure 6A). This cell population was characterized by an IL17$^+$ CD4$^+$ CD45$^+$ CD90$^+$ Sca1$^+$ CD44^{hi} CD27^{lo} CD23R^{hi} phenotype (Figure 6B). When the analysis was extended to cells from T-*Il2*$^{-/-}$ or *Il2*$^{-/-}$ mice, there was no expansion of the Th17 subset, in marked contrast to DC-*Il2*$^{-/-}$ mice (Figure 6C). The phenotype of the expanded IL-17-producing population in DC-*Il2*$^{-/-}$ mice is reminiscent of IL-17$^+$ T memory stem cells, which have self-renewal potential and a stem-cell-like signature characterized by β-catenin accumulation (Luckey and Weaver, 2012; Muranski et al., 2011), and it is notably distinct from that of the CD4$^-$ IL-23$^+$-responsive innate lymphoid population with colitogenic properties found in *Rag*$^{-/-}$ mice (Buonocore et al., 2010). Although IL-17$^+$ T memory stem cells express markers of terminally differentiated T cells, they are long lived and maintain a molecular signature in line with their stem-cell-like nature (Muranski et al., 2011). This suggested that DC-derived IL-2 preserves Th17 plasticity while favoring the generation of terminally differentiated cells that will not amplify or perpetuate the acute inflammatory condition.

To confirm that Th17 plasticity contributed to the pathogenic profile of T cells primed with DC-*Il2*$^{-/-}$ cells, we investigated whether Th17 cells differentiated under conditions of IL-2 deficiency exhibited the pathogenic signature that has been associated with immune pathology across several settings (Lee et al., 2012). Within these settings, IL-23 contributes to the emergence of pathogenic Th17 effector cells (Wu et al., 2013). We measured mRNA levels of a panel of 13 markers (Table S2) in T cells, including surface receptors, nuclear receptors, transcription factors, and cytokines that have been associated with the pathogenic Th17 signature described above (Korn et al., 2009; Muranski et al., 2011; Wu et al., 2013; Yosef et al., 2013). T cells from immunized mice differentiated in co-culture with CD103$^+$ DCs deficient in IL-2 exhibited higher expression of T-cell-factor-encoding gene 1 (*Tcf7*), a transcription factor downstream of the Wnt-signaling pathway that regulates hematopoietic stem cell self-renewal and T cell development (Reya et al., 2003), as well as of *Il23r*, *Il17*, *Tnsf11*, *Tgfb3*, and *Ctnnb1*, relative to cells cultured with IL-2-competent DCs (Figure 6D). We then went on to conduct comprehensive gene expression analysis on IL-17-producing cells from the CD45$^+$ CD90$^+$ T cell compartment of *Aspergillus*-infected mice. This confirmed that the same Th17 pathogenic signature, with the known markers of T cell stemness, was expressed to a greater extent in ex vivo T cells from DC-*Il2*$^{-/-}$ mice relative to their WT counterparts (Figure 6E). Thus, IL-17$^+$ T memory stem cells expanded in DC-*Il2*$^{-/-}$ mice exhibited a pathogenic signature, with a prominent involvement of IL-23.

Aspergillus-Induced NFAT-Dependent IL-2 and IL-23 Production by CD103$^+$ DCs Regulates CD4$^+$ T Cell Functionality

To further assess the ability of lung DCs to contribute to the pathogenic signature of Th17 cells in the absence of IL-2, we asked whether lung CD103$^+$ DCs would produce IL-23 in addition to IL-2 in response to *Aspergillus* particles. Preliminary in vivo data indicated that CD103$^+$ DCs did express both *Il2* and *Il23* in response to *Aspergillus* (Figure 7A). Microarray expression analysis in WGP-particle- or A-sw-treated D1 cells showed that DCs upregulated *Il2* and *Il23* as well as *IL12b* (Figures 7B and S6A). We have recently shown that NFATc2 in D1 cells mediates epigenetic modification of DC cytokine and chemokine genes, including *Il2*, *Il23*, and *IL12b*, leading to their transcriptional expression (Yu et al., 2015). Therefore, we investigated whether lung CD11b$^+$ and CD103$^+$ DCs also activate these genes in response to fungal stimulation and the possible involvement of CnB1 (Figure S6B). Both subsets of DC increased their expression of *Il2*, *Il23*, and *IL12b* in response to A-sw, but this only depended on CnB1 in the case of CD103$^+$ DCs (Figure S6B). Therefore, we exposed T cells from immunized mice to recombinant IL-2 and IL-23 to clarify their roles in T cell differentiation and plasticity. Using in-vitro-activated CD4$^+$ T cells, we found that increasing amounts of exogenous IL-2 reduced *Il17* expression, whereas recombinant IL-23 increased *Il17* and *Tcf7* transcripts, both of which characterize the stem-cell-like Th17 phenotype (Figure 7C).

To explore the mechanisms underlying DC-IL-2-mediated Th17 polarization, we began by examining activation of the STAT family of transcription factors. Whereas IL-2 drives activation of STAT5, IL-23 induces phosphorylation of STAT3. The balance between pSTAT5 and pSTAT3 in activated T cells is a crucial determinant of T cell differentiation (Stockinger, 2007). STAT3 is also implicated in the emergence of stem-cell-like features as it is one of the processes regulated by Wnt/β catenin signaling, and it may also positively regulate β-catenin expression itself (Ibrahem et al., 2014; Zhang et al., 2014). Culturing CD4$^+$ T cells from CCFA-immunized mice with recombinant IL-2 and IL-23 revealed that IL-23 reduced the activation of STAT5 while increasing STAT3 activation, leading to accumulation of β-catenin in T cells and IL-17 release (Figure 7D). Similarly, on co-culturing CD4$^+$ T cells from immunized mice with GM-DCs from WT, *Il2*$^{-/-}$, or *Il23a*$^{-/-}$ mice that had been pre-incubated with CCFA and inactivated A-sw, we found that only *Il2*$^{-/-}$ DCs could drive the expansion of Th17 cells expressing abundant *Il17* and *Tcf7* transcripts (Figure 7E). Conversely, DCs from mice lacking the IL-23 p19 subunit were unable to differentiate into Th17 cells.

These data were further supported by in vivo findings. In pulmonary CD45$^+$ CD90$^+$ IL17$^+$ T cells from *Aspergillus*-infected mice, we found that mRNA expression of STAT3 and β-catenin was elevated in T cells of DC-*Il2*$^{-/-}$ mice relative to WT mice, indicating a major control of DC-derived IL-2 on T cell plasticity (Figures 7F and 7G). The absence of IL-2 in DCs in T cell

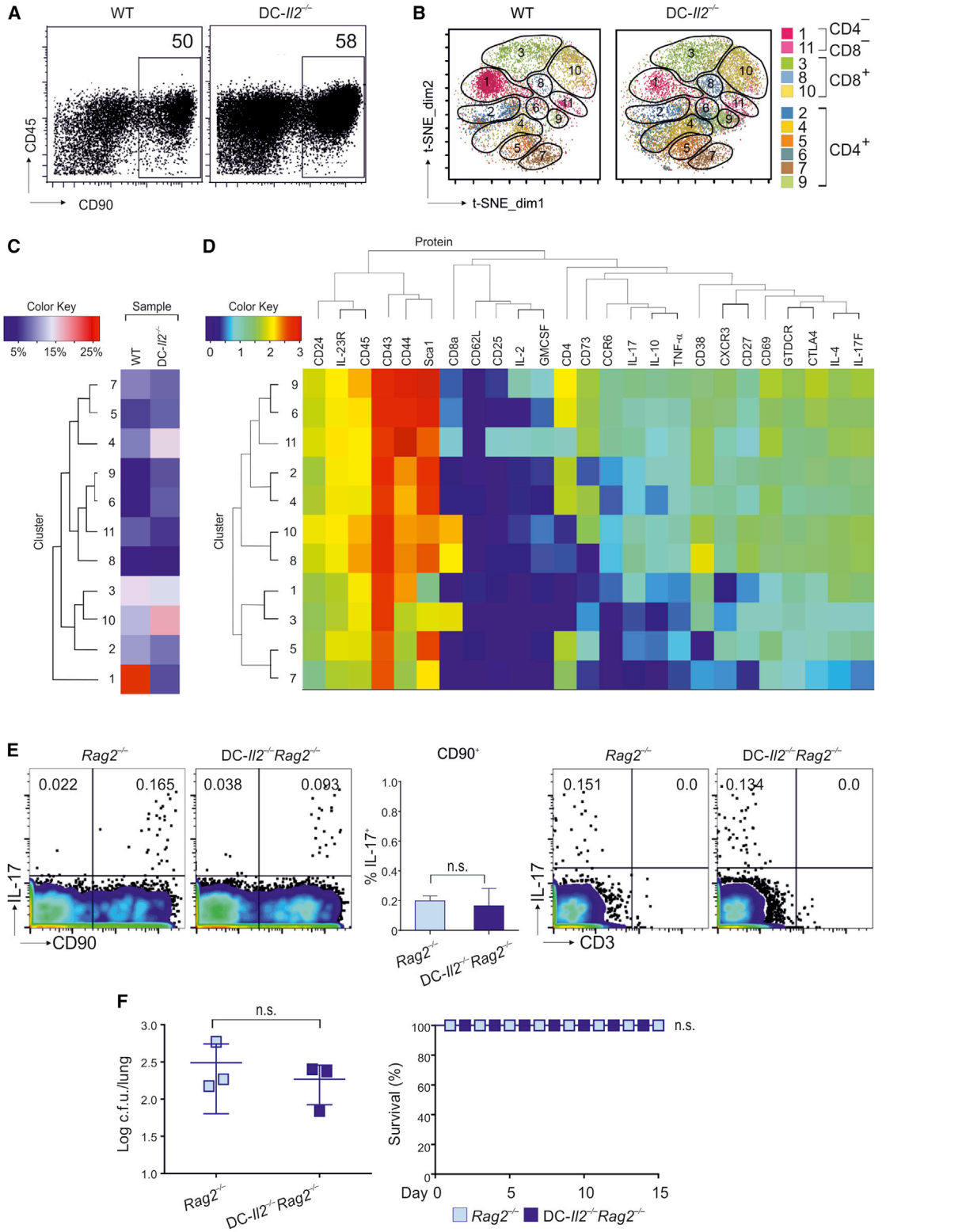

Figure 5. High Dimensional Analysis of Lung T Cell Subsets in the Absence of DC-Derived IL-2

WT, DC-*Il2*$^{-/-}$, *Rag2*$^{-/-}$, or DC-*Il2*$^{-/-}$ *Rag2*$^{-/-}$ mice were inoculated intranasally with *Aspergillus* and cells analyzed after 7 days.

(A) Representative mass cytometry dot plots showing the frequency of CD90^{+} cells within the CD45^{+} lung population. This gating strategy was used for subsequent t-SNE analysis.

(legend continued on next page)

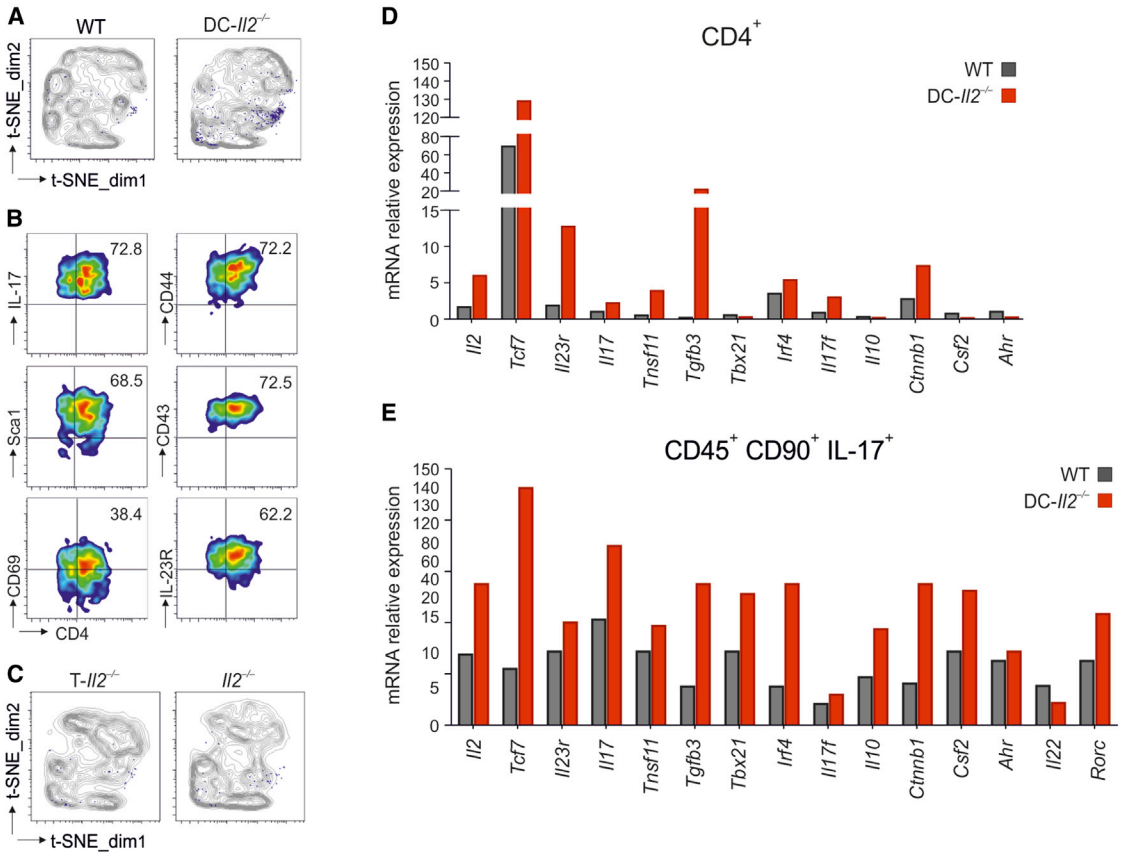

Figure 6. DC-Derived IL-2 Controls the Pathogenic Signature of Th17 Cells in *Aspergillus* Lung Infection

(A) Contour plots of mass cytometry data with IL-17A$^+$ cells (blue), gated and superimposed on the t-SNE map.

(B) Mass cytometry pseudocolor density plots on IL-17$^+$ CD45$^+$ CD90$^+$ cells from lungs of DC-*Il2*$^{-/-}$ mice.

(C) Contour plots of mass cytometry data with IL-17A$^+$ cells (blue), gated and superimposed on the t-SNE map.

(D) qRT-PCR in CD4$^+$ T cells isolated from lungs of CCFA-immunized mice co-cultured with lung CD103$^+$ DCs.

(E) qRT-PCR in IL-17$^+$ CD45$^+$ CD90$^+$ T cells isolated from lungs of mice inoculated intranasally with *Aspergillus* 7 days previously (means ± SD). Data are representative of three independent experiments (n = 9).

priming did not lead to increased transcription of DC *Il23* (Figure S6C). Because both IL-2 and IL-23 expression are dependent on CnB1 in CD103$^+$DCs and both cytokines contribute to regulating Th17 plasticity, the absence of CnB1 in DCs did not result in the development of lung pathology, increased IL-17 production, or higher susceptibility following *Aspergillus* intranasal infection (Figure S7). These results showed that the two cytokines exert distinct effects on CD4$^+$ T cell differentiation, with DC-derived IL-23 inducing a stem-cell-like molecular signature and a pool of memory stem cells that extends and amplifies the Th17 response, eventually leading to unrestrained inflammation.

DISCUSSION

IL-2 was discovered more than 30 years ago (Smith, 1988) and was initially studied for its T cell stimulatory properties, but it is now clear that it is at least as important for its regulatory roles (Yamanouchi et al., 2007). In our setting of invasive pulmonary fungal disease, the selective deficiency of IL-2 in DCs resulted in more-severe pathology and higher mortality than in WT mice or mice lacking IL-2 either in all CD4-expressing T cells or in all lymphoid tissues. Thus, the deletion of IL-2 in specific immune compartments can result in qualitative and quantitative differences in the immune response to pathogens. The absence or

(B) t-SNE map of CD90$^+$ CD45$^+$ lung cells color coded by DensVM automatically defined clusters and numbered as shown to compare the composition of WT and DC-*Il2*$^{-/-}$ mouse-derived T cell phenotypes.

(C) Heatmap of the frequencies of cells in each DensVM-defined cluster designated in (B).

(D) Heatmap of median intensities of each marker listed in Table S1 for cells in each cluster aggregated across WT and DC-*IL2*$^{-/-}$ mice. Data are representative of three independent experiments (n = 9 mice).

(E) Representative pseudocolor plots of IL-17 and CD90 or IL-17 and CD3 within CD45$^+$ lung cells population.

(F) *Aspergillus* CFU/lung (left panel; two-tailed Student's t test) and mouse survival rates (right panel) analyzed by log rank test (means ± SD).

See also Figure S5.

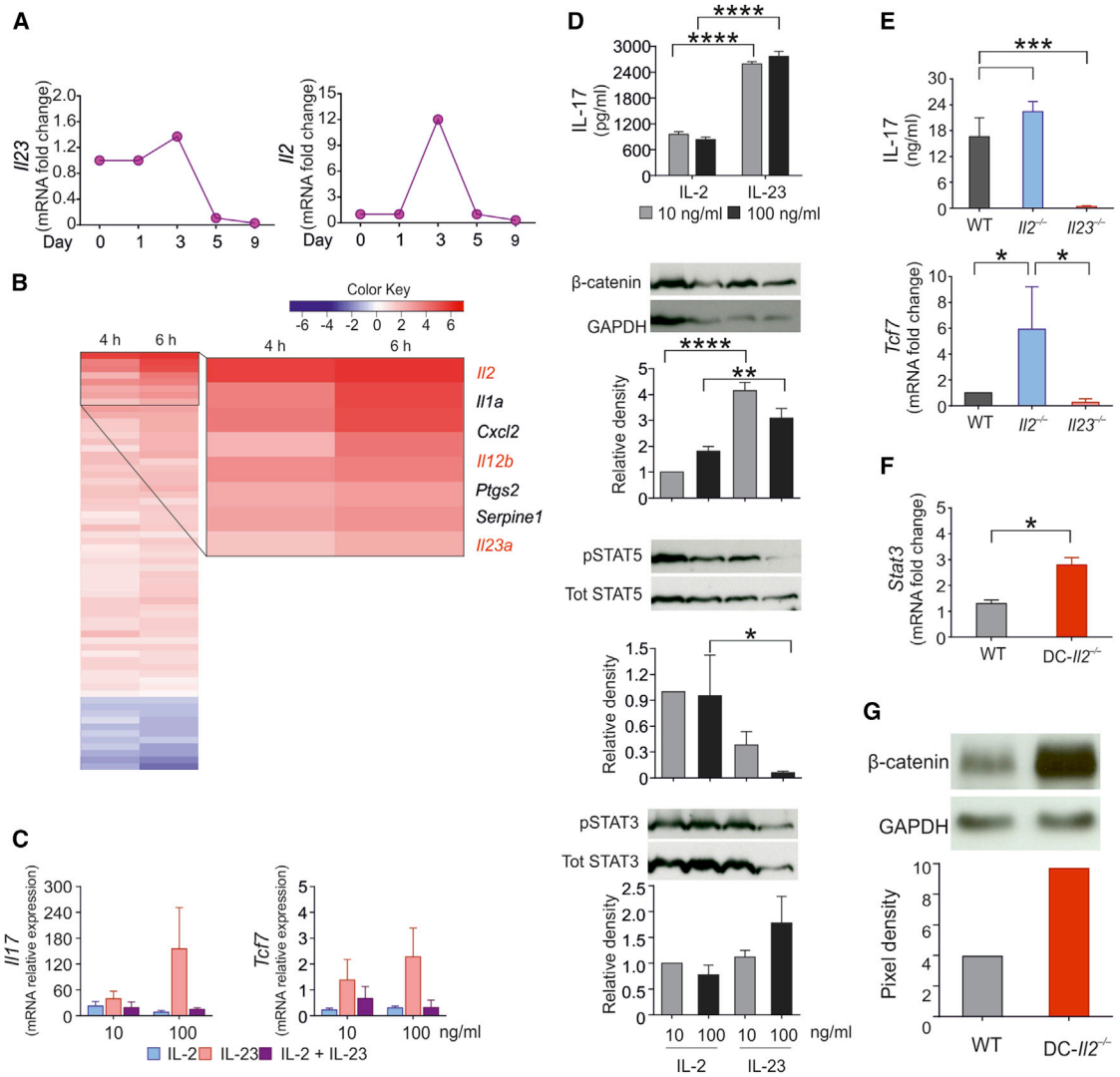

Figure 7. The Balance of IL-2 and IL-23 Production in DCs Regulates CD4⁺ T Cell Differentiation

(A) qRT-PCR of *Il2* and *Il23a* in sorted CD103⁺ DCs from lungs of uninfected WT (time 0) and *Aspergillus*-infected mice at the indicated days post-inoculation. Data are from one experiment representative of three.

(B) Microarray analysis of gene expression in A-sw-exposed D1 cells at the indicated time points, presented as a heatmap. Data are from one experiment representative of two.

(C) Real-time RT-PCR analysis of *Il17* and *Tcf7* in lung CD4⁺ T cells from uninfected WT mice after 3 days culture with recombinant mouse IL-23 and IL-2, followed by 4 hr stimulation with plate-bound anti-CD3 and soluble anti-CD28 antibodies under cytokine-neutral conditions (means ± SD).

(D) Western blot analysis of protein expression levels of pSTAT3, pSTAT5, β catenin, and IL-17 ELISA on CD4⁺ T cells from CCFA-immunized mice after cells were co-cultured with recombinant murine IL-2 or IL-23 at the indicated concentrations for 5 days. After 5 days, T cells were harvested and re-stimulated for 4 hr with recombinant cytokines. Plots refer to relative pixel density against total STAT3, total STAT5, and GAPDH, respectively (means ± SD). *$p < 0.05$, **$p < 0.01$, and ****$p < 0.0001$ (ANOVA with Bonferroni post-test).

(E) GM-DCs were incubated with heat-inactivated A-sw (cell-to-fungal morphotype ratio of 1:0.1) and CCFA (10 μg/ml) overnight. Thereafter, 1 × 10^6/ml CD4⁺ T cells were added at a ratio of 1 DC to 20 T cells. On day 6, supernatants were harvested and ELISA of IL-17 and qRT-PCR analysis of *Tcf7* were performed. Data are normalized to abundance of transcripts for the housekeeping gene *Gadph* and presented relative to WT mice. (means ± SD). *$p < 0.05$; ***$p < 0.001$ (ANOVA with Bonferroni post-test).

(F) qRT-PCR analysis of *Stat3* expression in IL-17⁺ CD45⁺ CD90⁺ T cells from lungs at 7 days post-infection (means ± SD).

(G) Western blot analysis of β-catenin in IL-17⁺ CD45⁺ CD90⁺ T cells at 7 days post-infection. Plots refer to relative pixel density against GAPDH.

Data are representative of three independent experiments; see also Figures S6 and S7.

substantially lower levels of IL-2 in *Il2*$^{-/-}$ and T-*Il2*$^{-/-}$ mice resulted in reduced frequency of T-reg cell and Foxp3 expression in the lungs and in peripheral lymph nodes, but DC-*Il2*$^{-/-}$ mice manifested increased numbers of IL-17-producing cells, which is known to correlate with a more-severe form of aspergillosis (Iannitti et al., 2013; Romani et al., 2008; Zelante et al., 2007).

We likewise observed that CD103$^+$ DCs appear a cellular source of IL-2 in the murine lung, adding another dimension to their established role in the response to particulate antigens (Greter et al., 2012). This implies that fungal morphotypes more enriched in β-glucan and capable of triggering phagocytosis—such as A-hyp or A-sw—are likely to be the primary inducers of the Ca^{2+}-calcineurin-NFAT pathway in lung CD103$^+$ DCs. In this regard, the concomitant release of IL-2 and IL-23 in our setting with ex vivo lung DCs in response to A-sw represents a regulatory process specifically instructed by CD103$^+$DCs in response to the fungus. From another perspective, fungi—because of their size and cell wall composition—may be a natural stimulus for instructing this regulatory response. Although we describe the phenotype of the pathogenic Th17 population in fungal infection, analogous results have been described in other settings (Antony and Restifo, 2002; Muranski et al., 2011), including GVHD, where an aberrant Th17 response contributes to disease maintenance (Zhang et al., 2005). The full range of scenarios in which this cell population is important remains to be explored.

There is strong evidence that human T cells can also be driven toward a Th17 phenotype under the direct influence of microbes (Zielinski et al., 2012), and therefore, there is a definite need for a better understanding of the potential for phenotypic diversity within this cell population in infection. We developed a 26-antibody panel for mass cytometry and used dimensionality reduction with machine-learning-aided cluster analysis to build a composite picture of murine lymphoid T cells during invasive pulmonary aspergillosis. Mass cytometry allowed us to establish that, in the absence of IL-2 from DCs, expansion of memory stem-cell-like IL-17$^+$ T cells is driven by IL-23 released by DCs in response to *Aspergillus*. IL-2 released by DCs is thus responsible for mitigating and controlling the pathogenicity of Th17 cells during the acute phases of pulmonary aspergillosis.

In investigating the mechanisms underlying emergence of the pathogenic Th17 population, we also revealed relationships between established immune modulators. β-catenin stabilization is known to exert a powerful effect on the prevention of inflammatory disease, yet we found that not only does it enhance survival of existing T-reg cells and promote unresponsiveness in precursors of T effector cells, but it also associates with the ability of IL-23 to differentiate and stabilize a pool of memory stem cells that represents a source of predominantly pathogenic Th17 cells.

We have recently conducted genome-wide mapping of NFATc2-binding sites in dectin-1-stimulated DCs and integrated our findings with gene expression data to identify the directly regulated targets of this transcription factor (Yu et al., 2015). DCs stimulated with curdlan revealed that NFATc2 translocates into the nucleus and regulates transcription of the genes—*Il2*, *Il12b*, and *Il23a*—that are required to produce heterodimeric IL-23. These results clearly demonstrate that fungi expressing high levels of β-glucan on their surface, as do the majority of fungal commensals, use NFAT to simultaneously activate transcription of both regulatory IL-2 and inflammatory IL-23. Thus, the ability of NFAT to respond to β-glucan particulates (Fric et al., 2014) represents an important evolutionary advantage because only the synchronized transcription of these genes (*Il2*, *Il12b*, and *Il23a*) leads to a non-pathogenic differentiation status of T cells in an anti-fungal immune response.

In summary, our study identifies a biologically relevant in vivo role for IL-2 production by DCs as well as a function for the Ca^{2+}-calcineurin-NFAT-IL-2-signaling pathway as a regulator of Th17 cell function. These data may pave the way for a renewed appreciation of the role of DC-derived IL-2 in immunity and inflammatory pathologies in the lung.

EXPERIMENTAL PROCEDURES

Mice

All experiments and procedures were approved by the Institutional Animal Care and Use Committee of Agency for Science, Technology and Research (A*STAR) (Biopolis) in accordance with guidelines by the Agri-Food and Veterinary Authority and National Advisory Committee for Laboratory Animal Research of Singapore. C57BL/6 mice and *Rag2*$^{-/-}$ mice were purchased from the Biological Resource Center, A*STAR. T-*Il2*$^{-/-}$ (Tg(Cd4-cre)1Cwi/BfluJ), *Il2*$^{-/-}$ (B6.C-Tg(CMV-cre)1Cgn/J), *Cnb*$^{fl/fl}$ (C57BL/6-Ppp3r1tm1Stl/J), *Cd11c*^{Cre} (B6.Cg-Tg(Itgax-cre)1-1Reiz/J), and ROSA26YFP (B6.Cg-Gt(ROSA)26Sortm3(CAG-EYFP)Hze/J) mice were purchased from JAX Mice and Services. Detailed information is reported in the Supplemental Experimental Procedures.

Statistical Analysis

The log rank test was used for paired data analyses of Kaplan-Meier survival curves. All in vitro determinations are means ± SD. Two-way ANOVA, Mann-Whitney, and unpaired t tests were performed using Prism 6.0 (GraphPad Software). All p values are two tailed.

ACCESSION NUMBERS

The accession number for the microarray data reported in this paper is GEO: GSE58590.

SUPPLEMENTAL INFORMATION

Supplemental Information includes Supplemental Experimental Procedures, seven figures, and three tables and can be found with this article online at http://dx.doi.org/10.1016/j.celrep.2015.08.030.

AUTHOR CONTRIBUTIONS

T.Z. designed the study and conducted and analyzed experiments; A.Y.W.W. did in vitro DC culture experiments, NFAT translocation luciferase assay, and graph editing; T.J.P. designed the method to analyze the efficiency of the deletion in DC-*Il2*$^{-/-}$, PCR, and qPCR experiments and performed lung DC sorting; J.C. performed the mass cytometry analysis; H.R.S. performed mass cytometry experiments; E.V. performed the Ca^{2+} entry assay; Y.H.B. designed and performed the ChIP assay; B.L. analyzed microarray data; F.Z. supervised the microarray experiments; J.F. carried out DC culture for microarray experiments; E.W.N. supervised the CyTOF experiments; A.M. supervised generation of mice with conditional deficiencies and the Ca^{2+} entry experiments; M.P. supervised the microarray analysis; T.Z. and P.P. wrote the manuscript; and P.R.-C. conceived and coordinated the project.

ACKNOWLEDGMENTS

This research was funded by the Biomedical Research Council, A*STAR. The authors wish to thank Lucy Robinson of Insight Editing London for assistance in manuscript preparation; S. Nabti for mouse colony maintenance; L. Mori for advice in mouse immunizations and B. Becher and M.C. Lafaille for advice in mouse screening strategies; A. Larbi, I. Low, and N. Binte Shadan at the Flow Cytometry Core Service, SIgN; B. Abel and A. Nardin from the Immunomonitoring platform, SIgN; G. Koh Jia Ling at the Functional Genomics Laboratory, SIgN; the IMCB Histopathology Lab, A*STAR; J.P. Abastado for experiments

on ROSA-YFP mice; Laurent Renia for *Myd88*$^{-/-}$ *Trif*$^{-/-}$ mice; and C. Massi-Benedetti for digital art and image editing.

Received: January 3, 2015
Revised: June 17, 2015
Accepted: August 7, 2015
Published: September 10, 2015

REFERENCES

Antony, P.A., and Restifo, N.P. (2002). Do CD4+ CD25+ immunoregulatory T cells hinder tumor immunotherapy? J. Immunother. *25*, 202–206.

Bandura, D.R., Baranov, V.I., Ornatsky, O.I., Antonov, A., Kinach, R., Lou, X., Pavlov, S., Vorobiev, S., Dick, J.E., and Tanner, S.D. (2009). Mass cytometry: technique for real time single cell multitarget immunoassay based on inductively coupled plasma time-of-flight mass spectrometry. Anal. Chem. *81*, 6813–6822.

Becher, B., Schlitzer, A., Chen, J., Mair, F., Sumatoh, H.R., Teng, K.W., Low, D., Ruedl, C., Riccardi-Castagnoli, P., Poidinger, M., et al. (2014). High-dimensional analysis of the murine myeloid cell system. Nat. Immunol. *15*, 1181–1189.

Boyman, O., and Sprent, J. (2012). The role of interleukin-2 during homeostasis and activation of the immune system. Nat. Rev. Immunol. *12*, 180–190.

Buonocore, S., Ahern, P.P., Uhlig, H.H., Ivanov, I.I., Littman, D.R., Maloy, K.J., and Powrie, F. (2010). Innate lymphoid cells drive interleukin-23-dependent innate intestinal pathology. Nature *464*, 1371–1375.

Fontenot, J.D., Rasmussen, J.P., Gavin, M.A., and Rudensky, A.Y. (2005). A function for interleukin 2 in Foxp3-expressing regulatory T cells. Nat. Immunol. *6*, 1142–1151.

Fric, J., Zelante, T., and Ricciardi-Castagnoli, P. (2014). Phagocytosis of particulate antigens - all roads lead to calcineurin/NFAT signaling pathway. Front. Immunol. *4*, 513.

Granucci, F., Vizzardelli, C., Pavelka, N., Feau, S., Persico, M., Virzi, E., Rescigno, M., Moro, G., and Ricciardi-Castagnoli, P. (2001). Inducible IL-2 production by dendritic cells revealed by global gene expression analysis. Nat. Immunol. *2*, 882–888.

Greter, M., Helft, J., Chow, A., Hashimoto, D., Mortha, A., Agudo-Cantero, J., Bogunovic, M., Gautier, E.L., Miller, J., Leboeuf, M., et al. (2012). GM-CSF controls nonlymphoid tissue dendritic cell homeostasis but is dispensable for the differentiation of inflammatory dendritic cells. Immunity *36*, 1031–1046.

Grünig, G., Corry, D.B., Leach, M.W., Seymour, B.W., Kurup, V.P., and Rennick, D.M. (1997). Interleukin-10 is a natural suppressor of cytokine production and inflammation in a murine model of allergic bronchopulmonary aspergillosis. J. Exp. Med. *185*, 1089–1099.

Guilliams, M., Ginhoux, F., Jakubzick, C., Naik, S.H., Onai, N., Schraml, B.U., Segura, E., Tussiwand, R., and Yona, S. (2014). Dendritic cells, monocytes and macrophages: a unified nomenclature based on ontogeny. Nat. Rev. Immunol. *14*, 571–578.

Hsu, Sf., O'Connell, P.J., Klyachko, V.A., Badminton, M.N., Thomson, A.W., Jackson, M.B., Clapham, D.E., and Ahern, G.P. (2001). Fundamental Ca2+ signaling mechanisms in mouse dendritic cells: CRAC is the major Ca2+ entry pathway. J. Immunol. *166*, 6126–6133.

Iannitti, R.G., Carvalho, A., Cunha, C., De Luca, A., Giovannini, G., Casagrande, A., Zelante, T., Vacca, C., Fallarino, F., Puccetti, P., et al. (2013). Th17/Treg imbalance in murine cystic fibrosis is linked to indoleamine 2,3-dioxygenase deficiency but corrected by kynurenines. Am. J. Respir. Crit. Care Med. *187*, 609–620.

Ibrahem, S., Al-Ghamdi, S., Baloch, K., Muhammad, B., Fadhil, W., Jackson, D., Nateri, A.S., and Ilyas, M. (2014). STAT3 paradoxically stimulates β-catenin expression but inhibits β-catenin function. Int. J. Exp. Pathol. *95*, 392–400.

Korn, T., Bettelli, E., Oukka, M., and Kuchroo, V.K. (2009). IL-17 and Th17 Cells. Annu. Rev. Immunol. *27*, 485–517.

Lee, Y., Awasthi, A., Yosef, N., Quintana, F.J., Xiao, S., Peters, A., Wu, C., Kleinewietfeld, M., Kunder, S., Hafler, D.A., et al. (2012). Induction and molecular signature of pathogenic TH17 cells. Nat. Immunol. *13*, 991–999.

Luckey, C.J., and Weaver, C.T. (2012). Stem-cell-like qualities of immune memory; CD4+ T cells join the party. Cell Stem Cell *10*, 107–108.

Malek, T.R. (2008). The biology of interleukin-2. Annu. Rev. Immunol. *26*, 453–479.

Muranski, P., Borman, Z.A., Kerkar, S.P., Klebanoff, C.A., Ji, Y., Sanchez-Perez, L., Sukumar, M., Reger, R.N., Yu, Z., Kern, S.J., et al. (2011). Th17 cells are long lived and retain a stem cell-like molecular signature. Immunity *35*, 972–985.

Newell, E.W., Sigal, N., Bendall, S.C., Nolan, G.P., and Davis, M.M. (2012). Cytometry by time-of-flight shows combinatorial cytokine expression and virus-specific cell niches within a continuum of CD8+ T cell phenotypes. Immunity *36*, 142–152.

Reya, T., Duncan, A.W., Ailles, L., Domen, J., Scherer, D.C., Willert, K., Hintz, L., Nusse, R., and Weissman, I.L. (2003). A role for Wnt signalling in self-renewal of haematopoietic stem cells. Nature *423*, 409–414.

Rogers, N.C., Slack, E.C., Edwards, A.D., Nolte, M.A., Schulz, O., Schweighoffer, E., Williams, D.L., Gordon, S., Tybulewicz, V.L., Brown, G.D., and Reis e Sousa, C. (2005). Syk-dependent cytokine induction by Dectin-1 reveals a novel pattern recognition pathway for C type lectins. Immunity *22*, 507–517.

Romani, L. (2011). Immunity to fungal infections. Nat. Rev. Immunol. *11*, 275–288.

Romani, L., Fallarino, F., De Luca, A., Montagnoli, C., D'Angelo, C., Zelante, T., Vacca, C., Bistoni, F., Fioretti, M.C., Grohmann, U., et al. (2008). Defective tryptophan catabolism underlies inflammation in mouse chronic granulomatous disease. Nature *451*, 211–215.

Schlitzer, A., McGovern, N., Teo, P., Zelante, T., Atarashi, K., Low, D., Ho, A.W., See, P., Shin, A., Wasan, P.S., et al. (2013). IRF4 transcription factor-dependent CD11b+ dendritic cells in human and mouse control mucosal IL-17 cytokine responses. Immunity *38*, 970–983.

Sharma, S., Quintana, A., Findlay, G.M., Mettlen, M., Baust, B., Jain, M., Nilsson, R., Rao, A., and Hogan, P.G. (2013). An siRNA screen for NFAT activation identifies septins as coordinators of store-operated Ca2+ entry. Nature *499*, 238–242.

Smith, K.A. (1988). Interleukin-2: inception, impact, and implications. Science *240*, 1169–1176.

Stockinger, B. (2007). Good for goose, but not for gander: IL-2 interferes with Th17 differentiation. Immunity *26*, 278–279.

Winzler, C., Rovere, P., Rescigno, M., Granucci, F., Penna, G., Adorini, L., Zimmermann, V.S., Davoust, J., and Ricciardi-Castagnoli, P. (1997). Maturation stages of mouse dendritic cells in growth factor-dependent long-term cultures. J. Exp. Med. *185*, 317–328.

Wu, C., Yosef, N., Thalhamer, T., Zhu, C., Xiao, S., Kishi, Y., Regev, A., and Kuchroo, V.K. (2013). Induction of pathogenic TH17 cells by inducible salt-sensing kinase SGK1. Nature *496*, 513–517.

Wuest, S.C., Edwan, J.H., Martin, J.F., Han, S., Perry, J.S., Cartagena, C.M., Matsuura, E., Maric, D., Waldmann, T.A., and Bielekova, B. (2011). A role for interleukin-2 trans-presentation in dendritic cell-mediated T cell activation in humans, as revealed by daclizumab therapy. Nat. Med. *17*, 604–609.

Yamanouchi, J., Rainbow, D., Serra, P., Howlett, S., Hunter, K., Garner, V.E., Gonzalez-Munoz, A., Clark, J., Veijola, R., Cubbon, R., et al. (2007). Interleukin-2 gene variation impairs regulatory T cell function and causes autoimmunity. Nat. Genet. *39*, 329–337.

Yosef, N., Shalek, A.K., Gaublomme, J.T., Jin, H., Lee, Y., Awasthi, A., Wu, C., Karwacz, K., Xiao, S., Jorgolli, M., et al. (2013). Dynamic regulatory network controlling TH17 cell differentiation. Nature *496*, 461–468.

Yu, H.B., Johnson, R., Kunarso, G., and Stanton, L.W. (2011). Coassembly of REST and its cofactors at sites of gene repression in embryonic stem cells. Genome Res. *21*, 1284–1293.

Yu, H.B., Yurieva, M., Balachander, A., Foo, I., Leong, X., Zelante, T., Zolezzi, F., Poidinger, M., and Ricciardi-Castagnoli, P. (2015). NFATc2 mediates epigenetic modification of dendritic cell cytokine and chemokine responses to dectin-1 stimulation. Nucleic Acids Res. *43*, 836–847.

Zanoni, I., Ostuni, R., Capuano, G., Collini, M., Caccia, M., Ronchi, A.E., Rocchetti, M., Mingozzi, F., Foti, M., Chirico, G., et al. (2009). CD14 regulates the dendritic cell life cycle after LPS exposure through NFAT activation. Nature *460*, 264–268.

Zelante, T., De Luca, A., Bonifazi, P., Montagnoli, C., Bozza, S., Moretti, S., Belladonna, M.L., Vacca, C., Conte, C., Mosci, P., et al. (2007). IL-23 and the Th17 pathway promote inflammation and impair antifungal immune resistance. Eur. J. Immunol. *37*, 2695–2706.

Zelante, T., Fric, J., Wong, A.Y., and Ricciardi-Castagnoli, P. (2012). Interleukin-2 production by dendritic cells and its immuno-regulatory functions. Front. Immunol. *3*, 161.

Zhang, Y., Joe, G., Hexner, E., Zhu, J., and Emerson, S.G. (2005). Host-reactive CD8+ memory stem cells in graft-versus-host disease. Nat. Med. *11*, 1299–1305.

Zhang, P., Li, H., Yang, B., Yang, F., Zhang, L.L., Kong, Q.Y., Chen, X.Y., Wu, M.L., and Liu, J. (2014). Biological significance and therapeutic implication of resveratrol-inhibited Wnt, Notch and STAT3 signaling in cervical cancer cells. Genes Cancer *5*, 154–164.

Zielinski, C.E., Mele, F., Aschenbrenner, D., Jarrossay, D., Ronchi, F., Gattorno, M., Monticelli, S., Lanzavecchia, A., and Sallusto, F. (2012). Pathogen-induced human TH17 cells produce IFN-γ or IL-10 and are regulated by IL-1β. Nature *484*, 514–518.